Journal of Polymers and the Environment
https://doi.org/10.1007/s10924-024-03478-0

ORIGINAL PAPER

Structural Characterization of Microcapsules from Common Bee Pollen for the Development of Delivery Systems

Seymanur Ertosun[1,2] · Volkan Aylanc[1,2,3] · Andreia F. Peixoto[2] · Arantzazu Santamaria-Echart[1] · Paulo Russo-Almeida[4] · Cristina Freire[2] · Miguel Vilas-Boas[1]

Accepted: 13 December 2024

Abstract

Exine, in the form of a natural microcapsule, refers to the outermost layer of the pollen grains and is composed of a complex mixture of sporopollenin, a highly resistant polymer, which makes it durable and able to withstand harsh conditions. Distinctive features of sporopollenin have attracted interest in the encapsulation of bioactive substances. Herein, we describe the pathway to producing sporopollenin microcapsules (SMCs) by exploiting bees and trapping common bee pollen pellets, offering a simple approach to acquiring substantial amounts of pollen grains for industrial application. Palynological results showed that separating bee pollen pellets by colour could lead to almost pure products ranging from 90 to 96%, depending on the pollen species. Subsequently, a single extraction technique removed around 82– 86% of the proteinaceous content, which could cause potential allergic reactions in humans. Detailed morphological analysis by scanning electron microscope (SEM), confocal laser scanning microscopy (CLSM), atomic force microscopy (AFM), and laser diffraction particle size (LDPS) analysis proved that the purified SMCs retained their 3D micro-structures, besides being hollow and uniform micron-scale size. Fourier-transform infrared spectroscopy (FTIR) findings point out that the sporopollenin biopolymer structure of the pollen grain comprises distinct aliphatic and aromatic domains, and the purification of the SMCs resulted in the loss of nitrogen-related peaks. The hydrophobic/hydrophilic properties of the SMCs, evaluated by contact angle measurements, showed variability between pollen, depending on the specificities of their chemical structure. Simultaneous thermal analysis (STA) confirmed SMCs thermal stability up to 451 °C. Altogether, we showed that green microcapsules with various morphological properties could be produced by simply processing *Castanea* spp., *Cistus* spp., *Erica* spp., *Olea* spp, and *Rubus* spp, all common bee pollen pellets available in large quantities in the northeast of Portugal, but also many other countries. These microcarriers promise applicability to various fields, from pharmaceuticals to the food industry.

Keywords Bee Pollen · Sporopollenin biopolymer · Morphological characterization · Green carriers

✉ Miguel Vilas-Boas
mvboas@ipb.pt

1 CIMO, LA SusTEC, Instituto Politécnico de Bragança, Campus de Santa Apolónia, Bragança 5300-253, Portugal

2 Departamento de Química e Bioquímica, Faculdade de Ciências, LAQV-REQUIMTE, Universidade do Porto, Porto 4169-007, Portugal

3 PerMed Research Group, Center for Health Technology and Services Research (CINTESIS), Rua Doutor Plácido da Costa, Porto 4200-450, Portugal

4 Centre for the Research and Technology of Agro-environmental and Biological Sciences, Departamento de Zootecnia, CITAB; Laboratório Apícola– LabApis, Universidade de Trás-os-Montes e Alto Douro (UTAD), Vila Real 5000-801, Portugal

Introduction

Plant pollen is a powder-like substance produced by the male reproductive organs of flowering plants, and the primary function of pollen is to fertilise the female reproductive organs [1]. Pollen grains are typically tiny and lightweight, allowing them to be easily carried by various agents such as wind, water, or insects to reach the female reproductive structures of other plants [1]. Plant-based pollen grains, which are natural microcapsules, exhibit species-specific features such as surface protrusions, pores, size, and other surface decorations [2]. One of the main elements that enable pollen grains to perform their role in nature successfully is the pollen wall, which protects the genetic material

Published online: 19 December 2024

in the inner cavity [3]. The inner layer (intine) is composed of elastic, load-bearing cellulose/hemicellulose, pectin, and microfibrils, while the outer layer (exine) is composed of sporopollenin, a robust and cross-linked biopolymer [4]. This double-layer wall provides a highly durable and chemically resistant protective barrier for pollen grains [5–7]. It forms a harsh, resistant coat that shields the cellular material inside from various environmental stresses such as desiccation, UV radiation, temperature extremes, and microbial and chemical degradation [3, 4].

All these features make sporopollenin particles good candidates for employing as encapsulation structures, SMCs, in the design of carrier systems [7–9]. Apart from the protective function of sporopollenin as an inherent natural microcapsule, it has been intensively researched in various research fields due to its naturally abundant and sustainable natural source [10–12]. Moreover, another interesting point of using SMCs is that they offer some distinctive advantages over synthetically produced microcapsules [2, 9]: (i) no need to redesign for the production of micro-sized structures, (ii) fewer chemicals and complicated devices are needed, (iii) species-specific uniformity dispersion, and (iv) biodegradable and non-toxic. SMCs purified from various pollen species make them a theme of interest as natural materials, particularly for their performance in the encapsulation and delivery of therapeutic agents such as drugs [6], vaccines [8], proteins [13] and living cells [5], besides their use in food sciences [14], energy storage systems [15], separation technology [10], catalytic reaction [16], and colloidal science and cellular applications [17].

Even though SMCs isolated from pollen grains are generally collected directly from plants, few published studies have reported that they may also be extracted from bee pollen pellets [18–20]. In fact, purifying SMCs from bee pollen pellets may offer some benefits, such as obtaining pollen types of various morphologies in a short time from a single location (apiary or hives) [9], particularly in those cases where the pollen is well appreciated by honeybees, allowing to acquiring substantial amounts of pollen for industrial application. Bees visit the flowers to collect pollen grains and blend them with some nectar and their own secretions into moist pellets so they can be carried to the hive stocked to the pollen basket on their hind legs [1, 21]. If a pollen trap is placed at the hive's entrance, the bee pollen pellet will be detached from the honeybee's hind legs, falling into the stock compartment of the pollen trap, allowing its diary collection, Fig. 1. Bee pollen pellets are 3–5 mm in size with 15 mg weight, and each pellet consists of thousands of pollen grains, usually from the same plant origin [1, 21], so this is the key point for efficiently producing SMCs with uniform size distribution and desired morphological characteristics.

Inspired by the fact that the pollen wall is a subject of interest and research in various research fields, herein we provide a straightforward pathway to collect pollen grains from common plant species by exploiting bees, and then purify SMCs from these bee pollen pellets and characterize them in detail physically and chemically. Besides describing the full pathway production, we expand the range of natural materials that can be used for the sustainable development of delivery systems by introducing new pollen types of SMCs that are available in high quantities in nature.

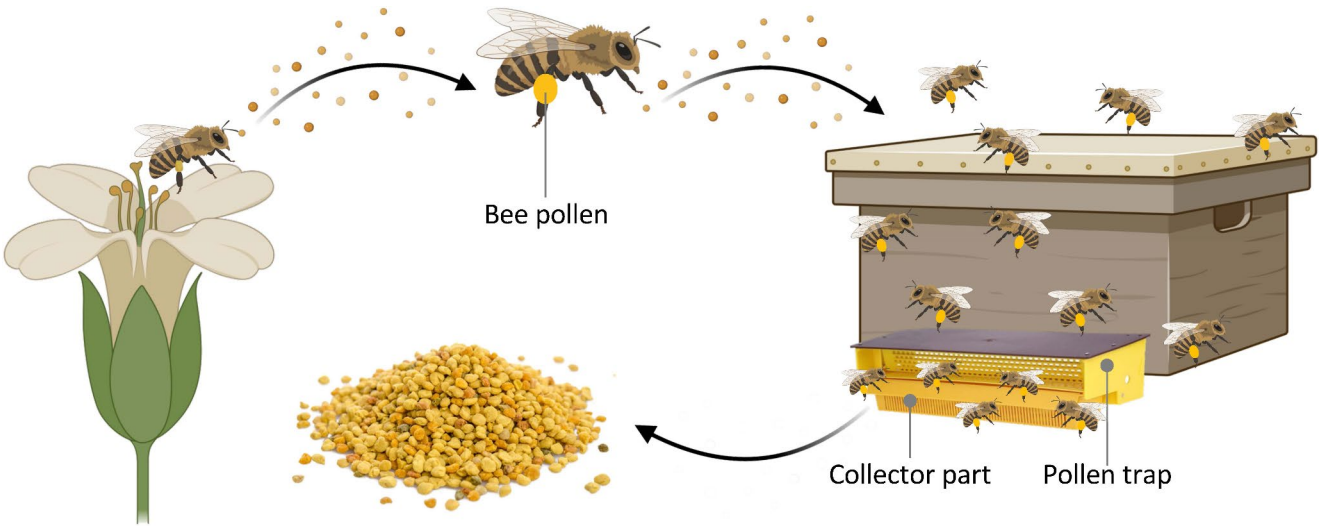

Fig. 1 The diagram visualizes the collection and pelletization of plant pollen by the bees, followed by the collection of bee pollen pellets that adhere to the bees' hind legs through pollen traps placed at the hive's entrance

Materials and Methods

Bee Pollen Collection and Processing

Bee pollen samples were collected using *Apis mellifera iberiensis* hives in Bragança (Portugal) between March and August 2022 (see Table S1), according to the blooming time of the plant, giving the desired pollen species. Samples were obtained by placing pollen traps on the hive entrance and collecting the pollen samples every two days. The harvested bee pollen pellets were cleaned from wood residues and dead bee parts and examined under a light microscope to identify each colour's pollen species. Following this step, pollen pellets of interest were separated by shape and colour under daylight. Approximately 50 g of pollen, per pollen species, was gathered to conduct all assays. The percentage of bulk bee pollen necessary to achieve the specific pollen amount was variable depending on the pollen type and time of collection but varied between 200 and 500 g. Selected bee pollen pellets were stored at − 22 °C until further analysis.

Palynological Analysis

The palynological analysis was carried out to reveal the plant origins of bee pollen samples previously separated by colour. Briefly, 20 mL of water was added to 2 g of bee pollen pellets in a Falcon tube, then vigorously mixed to make a homogeneous disaggregate sample and allow a representative sub-sample. An aliquot of 0.4 mL of the resulting mixture was centrifuged at 3500 rpm for 15 min. The resulting pellet was subjected to acetolysis, as previously reported [22]. Pollen identification and counting were accomplished by using an optical microscope (Nikon Microphot-FXA, Nikon Co., Tokyo, Japan). As recommended, more than 1000 pollen grains were counted per preparation, according to Van der Ohe et al. [23].

Extraction of SMC from Bee Pollen

A purification method consisting of two main steps was applied to obtain SMCs from each type of bee pollen [19, 20]. In the first step, defatting, 50 g of bee pollen was refluxed in 400 mL of acetone (50 °C, 250 rpm) for 3 h. After pouring the supernatant, the sample was mixed twice with 400 mL of warm water (50 °C, 250 rpm) in 1-hour periods until obtaining individual particles. After the washing step, the sample was refluxed in 400 mL of acetone (50 °C, 250 rpm) for 3 h, and the acetone was decanted. The sample was allowed to air dry in a fume hood for 12 h. The dried sample was stirred in 400 mL of diethyl ether (room temperature (RT), 300 rpm) for 2 h. After vacuum filtration, the same step was repeated with the same portion of fresh diethyl ether. Using a magnetic stirrer, the sample was stirred overnight in 400 mL of fresh diethyl ether (RT, 300 rpm). After removing the supernatant, the sample was left to dry in a fume hood for 12 h.

In the second step, acidolysis, the defatting samples were subjected to 400 mL 85% (w/w) phosphoric acid (70 °C, 330 rpm) for 8 h. After acidolysis, the samples were subjected to a series of washes consisting of 400 mL portions set at 50 °C: water (×5), acetone (×2), 2 M hydrochloric acid (×1), 2 M sodium hydroxide (×1), water (×5), acetone (×1), ethanol (×2) and water (×1). Finally, extracted SMCs were transferred to a glass Petri dish and dried in an oven (Memmert UNE400, Schwabach, Germany) at 45 °C for three days. Throughout the purification method, samples were collected by vacuum filtration system (Model DA7C, Charles Austen Pumps Ltd., Byfleet, UK).

Total Protein Content Analysis

A Kjeldahl steam distillation unit (Pro-Nitro A, JP Selecta, Barcelona, Spain) was used with a minimum of 250 mg sample to determine the protein content of both treated and untreated samples. The total protein content was calculated from the percent nitrogen multiplied by the factor of 6.25, which aligns with the recommendations of the Association of Official Analytical Chemists [24].

Morphological Imaging Analyses

Scanning Electron Microscope

Changes in the surface structure before and after chemical treatment were observed with an FEI Quanta 400 FEG ESEM/EDAX Genesis X4M (FEI Inc., OR, USA) instrument at 15.00 kV acceleration voltage under various magnifications. For capturing images, samples were spread on conductive carbon tapes and coated with Au/Pd using sputter coater equipment (SPI Module Sputter Coater, PA, US) (15 mA, 100 s).

Confocal Fluorescence Imaging

Since the sporopollenin wall of pollen is of an autofluorescence nature, it allowed the observation of both treated and untreated pollen grains using confocal laser scanning microscopy (CLSM). Samples were spread on a glass slide with a drop of epifluorescence mounting medium (Vectashield®, Vector Laboratories, CA, USA) containing 4'−6-diamidino-2-phenylindole (DAPI), mounted with a coverslip and stored in the dark at 4 °C until observation. LSM 510 META with a Zeiss Axio Imager Z1 (Carl Zeiss, Oberkochen, Germany) and the LSM 510 software

(version 4.0 SP2) were used to acquire confocal images. The same settings were applied to all images to normalize the results. The lasers used were argon (488 nm) set at 13%, helium-neon (543 nm) set at approximately 51%, and diode (405 nm) set at approximately 39%. The pinhole was set to 96 mm (1.02 airy units) for the argon laser, 102 mm (0.98 airy units) for the helium-neon laser, and 112 mm for the diode laser using a 63× objective. Images were captured at a scan speed of 6 or 8 with 1 µm thick Z sections, deconvolutioned using the 3D deconvolution tool of the AutoQuant X3 software (Media Cybernetics), and processed in TIFF images with ImageJ (1.47v).

Atomic Force Microscopy

Atomic force microscopy (AFM) imaging was performed on SMCs purified from the different pollen species. Samples were fixed to a flat mica surface using a commercially available nail polish brand (Golden Rose, Istanbul, Turkey) based on nitrocellulose and polyvinyl butyral resin [12]. AFM imaging was carried out at room temperature (21 °C) in tapping mode using an AFM model TT-AFM (AFM Workshop, SC, USA) instrument equipped with a nominal tip radius < 10 nm (ACT, AppNano, CA, USA) with a resonance frequency of around 300 kHz. Images were preprocessed using Gwyddion 2.4 software.

Laser Diffraction Particle Size Analysis

Measurement of the particle size of the SMCs was performed using a Mastersizer 3000 (Malvern Panalytical Inc., Malvern, UK) based on the laser diffraction technique [25]. Samples were analysed by taking an average of 5 measurements at 21 °C using distilled water as the dispersion medium. The determined parameters were D_{10}, D_{50}, and D_{90}, in volume, which denoted the particle size corresponding to 10%, 50%, and 90% of the total volume of the particles in the tested sample, respectively.

Fourier-transform Infrared Spectroscopy

FTIR measurement was performed using the PerkinElmer Spectrum BX FT-IR system (Perkin Elmer Inc., MA, USA) equipped with a diamond attenuated total reflection (ATR) accessory (GladiATR, PIKE Technologies, WI, USA). Reflectance infrared spectra were collected at a spectral resolution of 4 cm^{-1} by 64 times scanning per measurement over the range from 4000 to 600 cm^{-1}. Background spectra were collected before the sample reading.

Contact Angle Measurement

For contact angle measurements, 50 mg of sample was pelleted (13 mm diameter, 5 tons pressure for 20 s) with an IR pelletizer to achieve a flattened surface and then fixed on a glass slide. A drop of water (3 µL at 21 °C) was gently dropped onto the surface of the SMCs layer. The contact angle was measured by filming and photographing using an Attension ThetaOptical Tensiometer (Biolin Scientific, Gothenburg, Sweden) with OneAttension 1.0 software.

Simultaneous Thermal Analysis

The thermal decomposition of treated and untreated samples was tested by thermogravimetric analysis (TGA), derivative TG (dTG), and differential thermal analysis (DTA) using the STA7200RV Simultaneous Thermal Analyzer System (Hitachi High-Tech Inc., Tokyo, Japan). Samples were heated from 20 to 700 °C at a scan rate of 10 °C/min. Data were processed using TA7000 software (Hitachi High-Tech Inc., Tokyo, Japan), version 11.1).

Data Processing

GraphPad Prism version 9.3 (San Diego, CA, USA) was employed for data analysis. Data were compared using a two-tailed *t*-test, and $p < 0.05$ was considered significant.

Results and Discussion

Isolation of SMCs From Bee Pollen

Using bee pollen pellets as a sustainable source to gather SMCs, isolate, and transform them into usable biomaterial seems an advantage over the direct pollen collection from flowers. For this purpose, we set the area (apiary) to collect bee pollen pellets based on the target plant flora and consider the appetence of honeybees for specific pollen grains, following local beekeepers' experience. The principle was to set the collection based on common pollen types that could be gathered in significant amounts and worldwide if we want to fulfill a future demand for industrial applications. Five pollen types were targeted *Castanea* spp., *Cistus* spp., *Erica* spp., *Olea* spp and *Rubus* spp. Once the colonies were established, the pollen traps were placed at the hive's entrance at predefined time intervals during the pollination period of the target plants so that enough sample could be collected, minimizing the impact on the colony's development. Samples gathered on different days were worked separately until confirmation of their botanical origin.

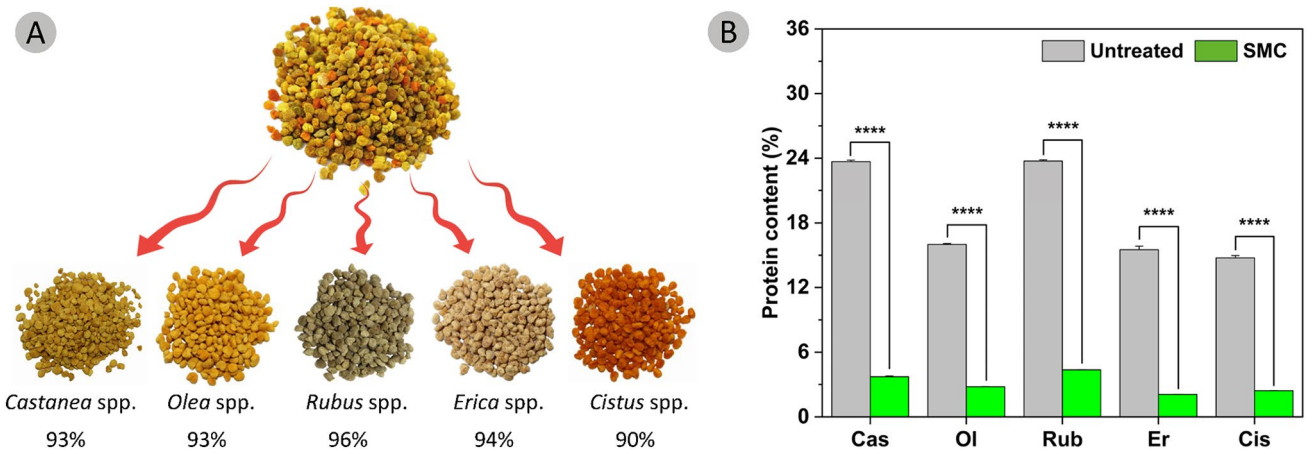

Fig. 2 Separation of collected bee pollen and nitrogen content analysis. (**A**) Photographs of bee pollen pellets separated by their color and morphology and their degree of purity were based on the results of palynological analysis, and (**B**) the total protein content was calculated by multiplying the nitrogen amount by a factor of 6.25. A two-tailed *t*-test was used for comparison. [****] = $p < 0.0001$

After collection, the samples were separated by the shape and colour of the pollen pellet and subject to palynological analysis to confirm the botanical origin and specify the purity of the bee pollen sub-sample. The results revealed purity values from 90 to 96%, so each colour represented a single plant species, Fig. 2. The deviation for total purity may result from moist pollen pellets coming into contact with each other as they fall into the collector part of the pollen traps rather than an event that occurs when bees form pollen pellets. To reduce this contamination, pollen residues on the surface of the pellets could be removed by lightly sieving after drying at a moderate temperature in an oven.

Once separated, the pollen grains were subjected to an extraction procedure consisting of defatting, acidolysis, and a series of washing to produce the SMCs. The SMCs were effectively isolated for all pollen species without further optimization. The purification weight yield of SMCs from raw bee pollen varied between 8.6 and 15.2%, depending on the species.

Determining the protein content of the SMCs, besides being an indirect measure of the efficient removal of the cytoplasmic content of the pollen grain, is essential for pharmaceutical and food use of the microcapsules because pollen proteins can cause allergies in some individuals [26]. When people with pollen allergies come into contact with pollen, their immune system may overreact and produce histamines, leading to allergic reactions such as sneezing, itching, watery eyes, and nasal congestion [13, 26]. We performed nitrogen analysis to quantify the total protein content of untreated bee pollen and SMCs. As given in Fig. 2, the total protein content of bee pollen was significantly ($p < 0.0001$, *t*-test) reduced from $23.7 \pm 0.1\%$ to $3.7 \pm 0.1\%$ in *Castanea* spp., or from $15.5 \pm 0.3\%$ to $2.1 \pm 0.5\%$ in *Erica* spp. These results agree with the findings reported for the protein content of other plants and bee pollen as raw sources for SMC extraction [4, 20]. Besides, some studies state that the chemical building blocks of the pollen wall containing nitrogen may affect the total protein content in SMCs [8, 26]. However, since the structure of sporopollenin has not been fully elucidated, the contribution of the amount of nitrogen it may contain to the total protein content has not been clearly demonstrated until now. Although the remaining protein content of SMCs would not be expected to cause potential allergic reactions, a full guarantee will require additional immunity assays using the serum of allergic individuals.

Table 1 Morphological features of isolated SMCs

SMCs	Shape	Surface ornamentation	Shape and aperture number	Diameter of apertures (μm)
Cas	Ellipse	Rugulate	Tricolporate; 3	1.4 ± 0.2
Ol	Spheroidal	Reticulate	Triporate; 3	1.8 ± 0.1
Rub	Triangular	Striate	Tricolporate; 3	Along the colpus
Er	Like-spheroid	Fossulate	Tricolporate; 3	1.4 ± 0.0
Cis	Spheroidal	Reticulate	Tricolporate; 3	3.1 ± 0.1

Cas: *Castanea* spp.; Ol: *Olea* spp.; Rub: *Rubus* spp.; Er: *Erica* spp.; and Cis: *Cistus* spp. (Cis)

Morphological Evaluation

Different analytical techniques such as SEM, CLSM, AFM, and LDPS were explored to investigate the isolated SMCs' morphological features compared with their original pollen grain. Each species-specific pollen grain has its own three-dimensional shape, surface architecture, and apertures located in the pollen wall, Table 1.

These unique morphological features of pollen grains can be damaged during their processing and prolonged treatment of SMCs with strong chemicals such as phosphoric acid [27]. SEM images evidenced that all SMC species' structural integrity was retained, and no deterioration was found in their surface architecture, Fig. 3. One of the slight changes observed was the shrinking of some microcapsules with the removal of their cytoplasmic contents, more evident in *Rubus* spp. Another change was the opening of the apertures by chemical treatment. In fact, the exine layer is very weak or absent in the areas where the openings are located and is usually composed of intine [26]. So, during the extraction of the pollen grains, the fluid enters into the pollen cavity via nanochannel, causing pressure, and it ends with the breakdown of the intine, which is weakened by the effects of chemicals (e.g., H_3PO_4) [9, 20]. These micro and nano apertures may actually be among the desired features for future loading of SMCs with different types of materials and their controlled release and/or delivery to predefined areas, e.g., in drugs, therapeutic nanostructures, food preservatives, etc [9, 14, 20, 26].

One of the main goals to be achieved when manufacturing SMCs is to obtain hollow structures and thus the benefit of the large inner cavity for various purposes. CLSM analysis is a great help in demonstrating that SMCs are free of cellular components. It is common knowledge that sporopollenin and raw pollen grains emit auto-fluorescence at organelle-specific wavelengths [13]. Taking advantage of this pollen property, we collected confocal microscopy images before and after chemical treatment, Fig. 4 and Figure S1. The pictures clearly show strong auto-fluorescence emitted in the inner cavity of the untreated raw pollen grains. Conversely, auto-fluorescence was not detected in the inner cavity of SMCs. These findings not only prove the successful removal of the cellular components of the pollen grains but also support the SEM results, which indicate that their 3D structures are retained.

To further characterize SMCs, we investigated the surface topography by AFM. Surface ornamentation is substantial when considering the intra-body use of SMCs because the nanoarchitecture on the surface of the exine layer can affect the adhesion, external surface chemistry, and mechanical properties of SMCs [7] and even generate an immune system response [28]. AFM analysis of raw bee pollen was unsuccessful due to the instability of residues on its surface. However, we could analyse SMCs since they underwent a series of chemical treatments and washing steps, Fig. 5. Therefore, we could only compare AFM images of SCMs with untreated and treated SEM images taken at high magnifications. AFM images show the exine wall in visible 2D slices (Fig. 5 upper line), however, the 3D images (Fig. 5 bottom line) provide a better understanding of the actual morphology of the exine.

Olea and *Cistus* exhibited reticulate surface ornamentation, whereas *Castanea* and *Rubus* displayed rugulate and striate surface ornamentation, respectively. On the other side, *Erica* possessed a distinct fossulate architecture, setting it apart from the other species in both morphology and exine ornamentation. The results evidenced that their 3D structure is preserved and has no significant deformations, but also offered notable information about both the structure and dimensions of the nano-architecture on the exine surface, as seen in Fig. 5. These results provide helpful information for the characterization of the SMCs surface nanoarchitecture and the development or modification of exine surfaces for further intentions.

The last analysis conducted on the morphological features of SMCs was the particle size distribution based on the laser diffraction technique, Fig. 6. Extracted Cas, Ol, Rub, Er, and Cis SMCs corresponded to mean spherical diameters of 12.5 ± 0.1 µm, 18.2 ± 0.1 µm, 18.5 ± 0.1 µm, 27.9 ± 0.1 µm, and 36.3 ± 0.1 µm, respectively. Depending on the pollen species, a diversity of particle sizes enables one to choose the microcapsule that better suits a desired volume. We also further characterized the values in the particle size distribution in volume (D_{10}, D_{50}, and D_{90}) for each SMC in Table S2. The particle distribution analysis and the evidence presented by SEM and CLSM analyses show that SMCs could be produced in different characteristics, such as hollow and monodisperse microstructures, where their structural integrity is preserved.

ATR-FTIR Analysis

FTIR spectroscopy was explored to evaluate the chemical composition of the raw bee pollen and purified SMCs and to understand the impact of the applied chemical treatment. The data, Fig. 7, was compared with the spectroscopic properties of untreated pollen grains and SMCs reported in the literature for various pollen species [29–36].

Alcohols, carboxylic acids, carbohydrates, phenols, or water exhibit ν(OH) oxygen-hydrogen vibrational mode [29]. For all bee pollen species, the broad band ν(OH) with a center of 3290 cm^{-1} is assigned to the vibrational mode in hydrogen bonding [36]. For SMCs, the peak is shifted to 3320 cm^{-1}, and a drastic decrease in intensity was observed. These displacements and structural changes are probably related to the removal of weakly bonded water, carbohydrates, or lipids, which are linked to $-$OH groups [35]. The peaks at 2928 and 2854 cm^{-1} in the spectra of bee pollen are due to the $\nu_{asym}(CH_2)$ and $\nu_{sym}(CH_2)$ modes of the methylene groups and remain at the same wavenumber in the isolated SMC, but the intensity of their absorption being

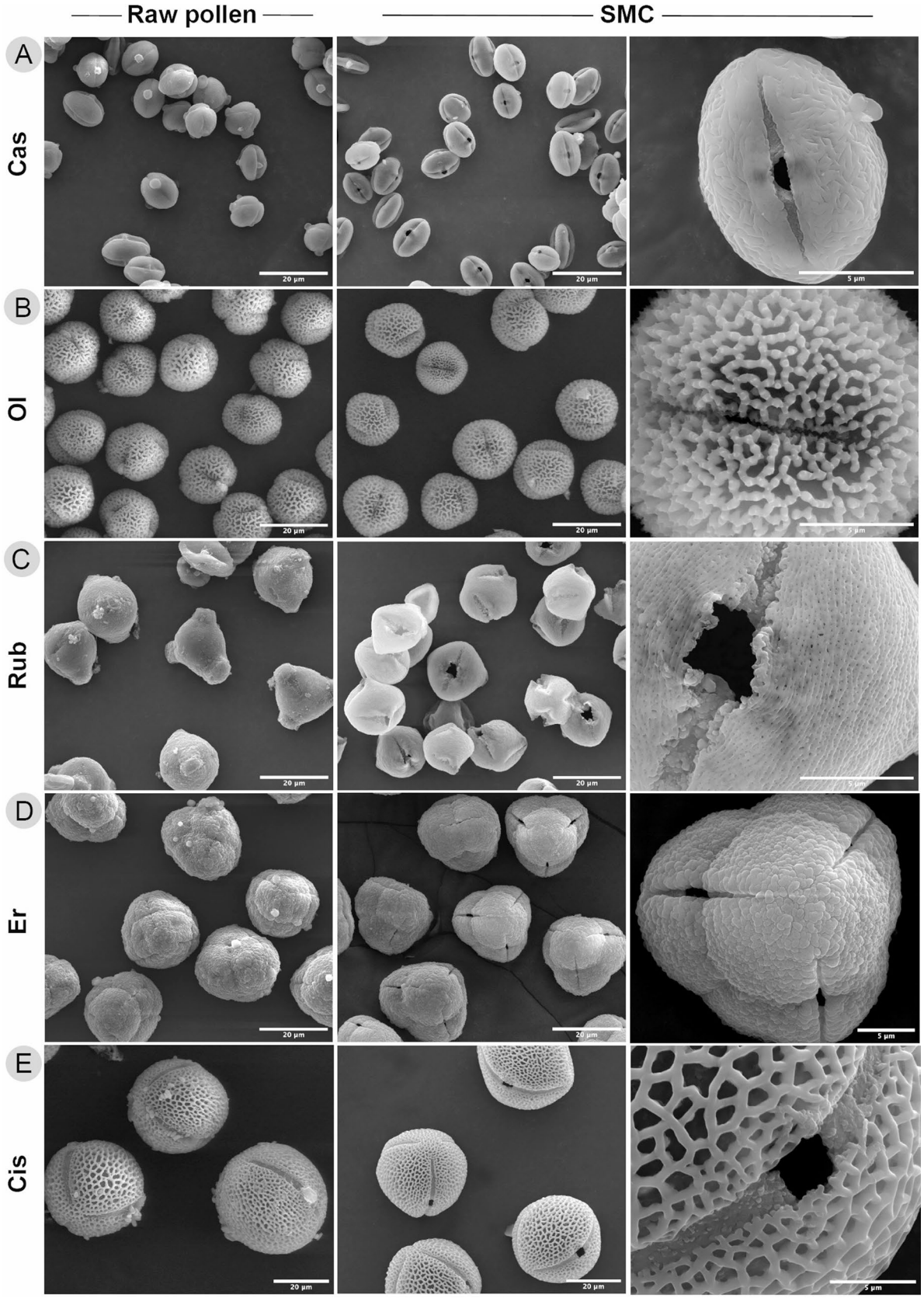

Fig. 3 Scanning electron micrographs for bee pollen (first column) and SMCs (second and third columns). (**A**) *Castanea* spp. (Cas), (**B**) *Olea* spp. (Ol), (**C**) *Rubus* spp. (Rub), (**D**) *Erica* spp. (Er), and (**E**) *Cistus* spp. (Cis)

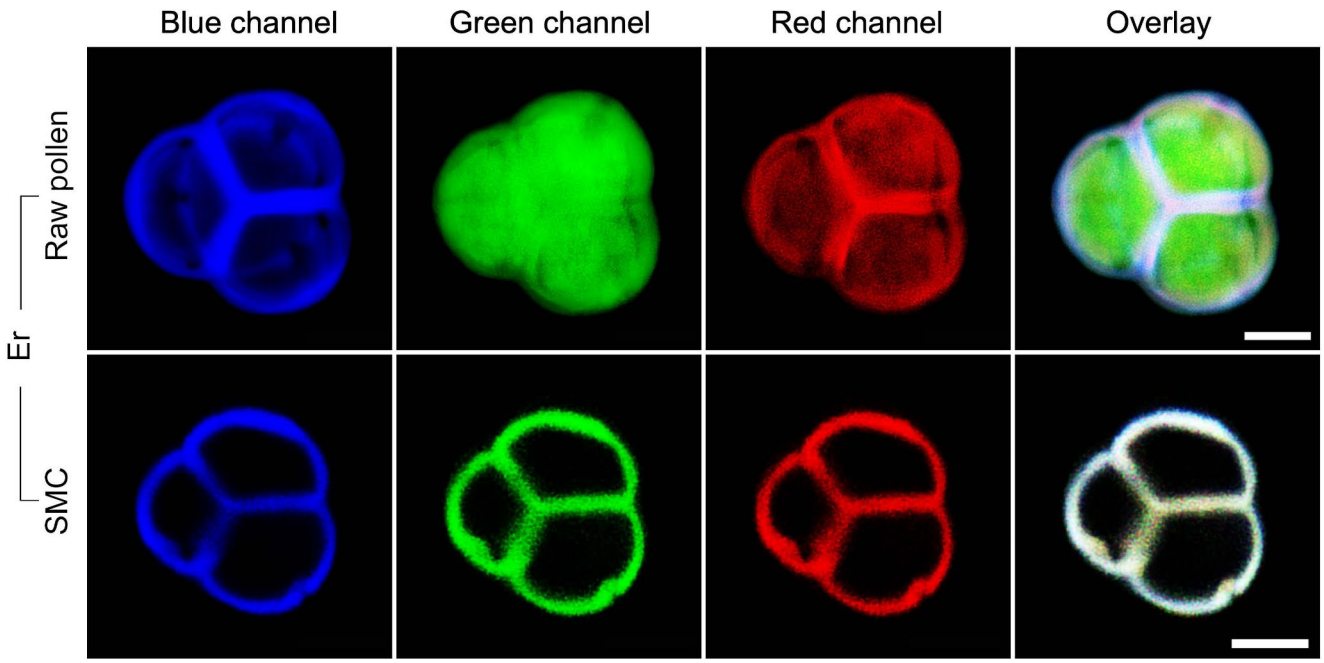

Fig. 4 Confocal micrographs of raw pollen (first row) and SMCs (second row) for *Erica* spp. (Er). Cytoplasmic native molecules and organelles of untreated pollen grains are clearly visible in blue, green, red, and overlay images. SMCs, which are treated pollen, retain the autofluorescence of the pollen wall, and it is clear that they are hollow. All confocal micrographs for other pollen species are given in the Supplementary Information; see Figure S1

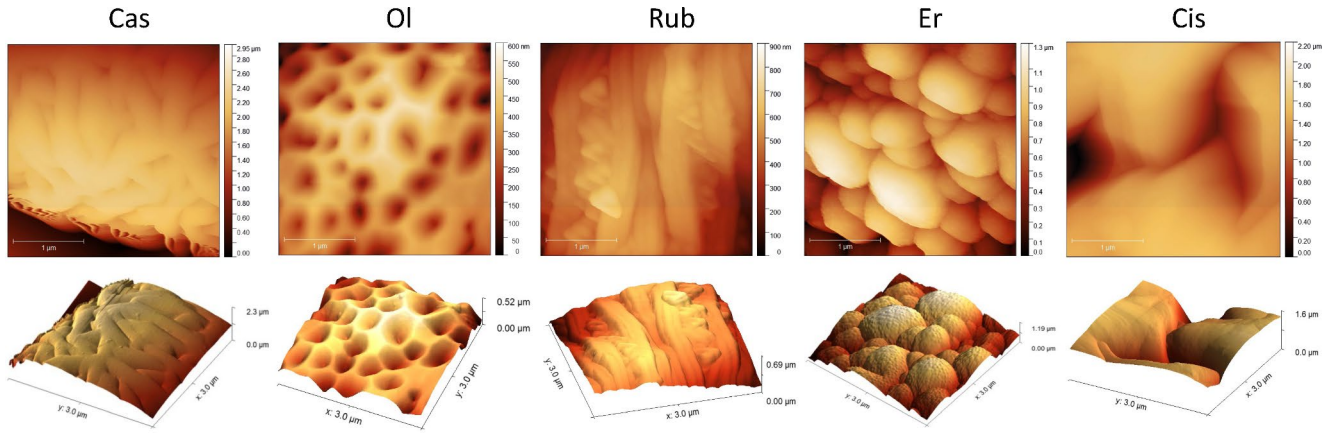

Fig. 5 AFM surface reconstructions were obtained over 3 µm × 3 µm areas. The upper line shows the AFM images of the various SMCs, and the lower row shows 3D surface reconstruction from height trace data from the same samples. Cas: *Castanea* spp.; Ol: *Olea* spp.; Rub: *Rubus* spp.; Er: *Erica* spp.; and Cis: *Cistus* spp. (Cis)

reduced [32, 33, 36]. Regardless of the isolated SMCs, raw pollen grains may contain natural lipids, carbohydrates, or proteins that exhibit carbon-oxygen or nitrogen-carbon vibrational modes. The peak at 1740 cm^{-1} appearing in the spectrum of bee pollen is attributed to the ν(C═O) mode of lipids [30]. Even though indisputable lipids are present in natural pollen grains, the hydrogen-bonded ν(C═O) mode of such compounds is manifested at lower frequencies [33, 34]. After treating raw pollen grains with organic solvents such as acetone and diethyl ether and the acidolysis step, it completely disappeared for SMCs, thus pointing out the removal of lipid content [36].

Spectra from raw bee pollen evidence the presence of amides. The peaks occurring around ~1636 cm^{-1} and at ~1548 cm^{-1} for the different types of pollen are assigned to ν(C═O) amide I and δ(NH), ν(CN) amide II, respectively

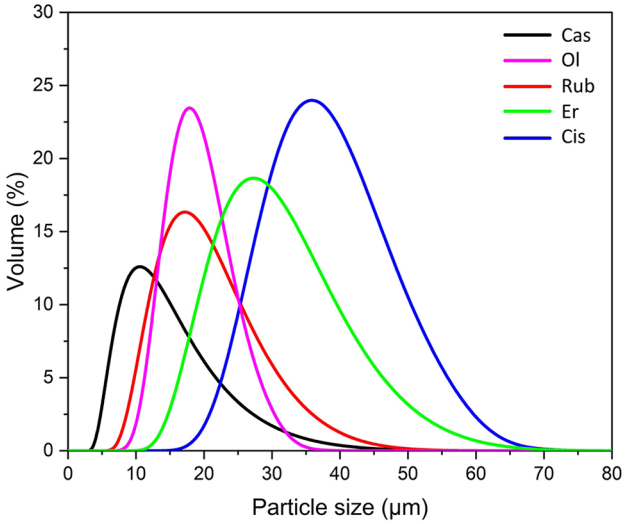

Fig. 6 Laser diffraction particle size analysis of SMCs obtained from different pollen species. Cas: *Castanea* spp.; Ol: *Olea* spp.; Rub: *Rubus* spp.; Er: *Erica* spp.; and Cis: *Cistus* spp. (Cis)

[32, 35]. For Rub, the presence of the amide II peak was not so evident, Fig. 7C. The well-defined peak at 1234 cm^{-1} is another evidence of this functional group and is assigned to the in-phase combination of δ(NH) and *ν*(CN) amide III [32, 35]. All these features assigned to the amide peaks, associated with the presence of proteins, disappeared after the chemical treatment. The peak at 1602 cm^{-1} that is distinguishable only in Cas bee pollen is due to the *ν*(C═C) aromatic ring modes, Fig. 7A [36]. Moreover, shoulders at ~1422 cm^{-1}, 1344 cm^{-1}, and 1040 cm^{-1} in the bee pollen spectrums are assigned $\delta_{scissors}(CH_2)$, $\gamma_{wagging}(CH_2)$ or methine deformation and polysaccharides (*ν*(COC), in cellulose), respectively [30, 33, 35]. After chemical treatment, there was a shift at ~1422 cm^{-1}, while the peaks at 1344 cm^{-1} and 1040 cm^{-1} disappeared. This suggests that phosphoric acid affected the carbohydrate backbone and likely removed cellulosic intine [35, 36].

On the other hand, the peaks observed around ~1654 cm^{-1} and ~1576 cm^{-1} in all purified SMCs are assigned to the *ν*(C═C) mode of alkenes and $\nu_{asym}(COO-)$ in the sporopollenin, respectively [29, 33, 35, 36]. The peak at 1434 cm^{-1} with the high positional consistency in SMCs has been previously assigned to δ(CH2) or δ(CH3) vibrations. Nevertheless, it could be attributed to the methylene $\delta_{scissors}(CH_2)$ mode based on the current findings from the sporopollenin [30, 33, 34]. In the spectra of isolated SMCs, the peak at 1092 cm^{-1} is consistent with the *ν*(CO) mode of secondary alcohols [30], and similar properties were reported in the cellulose (1100 cm^{-1}) and pectin (1100 cm^{-1}) spectra [33], hence the peak rising here is assigned to the *ν*(CO) mode of secondary alcohols or the *ν*(COC) mode of aliphatic ethers and may suggest polysaccharide residues [29, 35, 36]. However, these shoulders were not at an almost identifiable frequency in some species of SMCs (e.g., Ol, Er, and Cis), Fig. 7B and D, and 7E. The peak appearing at 990 cm^{-1}, which may be associated with residues of carbohydrates, is assigned to the *ν*(COC) mode [30, 35]. The peak around 840 cm^{-1} is probably a γ(CH) mode of the aromatic ring of the 1,4-disubstituted aromatic ring of *p*-Coumaric acid units [33]. Altogether, the spectra of the bee pollen pellets support the results of total protein and morphological imaging analysis, as well as the significant removal of carbohydrates, proteinaceous, and lipid components, which are part of their natural structure, after phosphoric acid chemical treatment. Besides, our ATR-FTIR findings point out that sporopollenin biopolymers comprise distinct aliphatic and aromatic domains.

Sessile-drop Contact Angle

Water interaction with surfaces is critical to biological, physical, and chemical phenomena [37]. Contact angle, an important parameter in the field of surface science and material characterization, provides valuable information about the wetting behaviour of the surface and the potential use of the material in the desired application. We used the contact angle θ as a measure of the wetting degree or the SMC surface by water, using the sessile drop method, Fig. 8.

Although the samples went through the same series of processes, there were some important differences among them. Cis SMCs exhibited the highest contact angle with a value of 112° ± 3 and Ol SMCs had the lowest with a value of 73° ± 3. This means that Ol SMCs have higher hydrophilic behaviour while Cis SMCs have hydrophobic properties. In fact, these two specimens have distinct surface ornamentations, microreticulate for *Olea* spp. and striate-reticulate for *Cistus* spp., and, most probably, differences in their chemical structure. When we referred to the FTIR results to understand the phenomenon, the areas with peaks 3290 cm^{-1}, 1576 cm^{-1}, and 1092 cm^{-1}, which are associated with the presence of OH, COO^- and CO functional groups, were relatively more significant in the Ol SMCs. Cas and Rub SMCs, which have a smoother surface than the other samples, exhibited hydrophobic behaviour with close contact angle values. The water contact angle findings evidenced significant changes in the water affinity of the SMCs depending on pollen species. Moreover, some reports demonstrated that the interaction of SMCs with water can

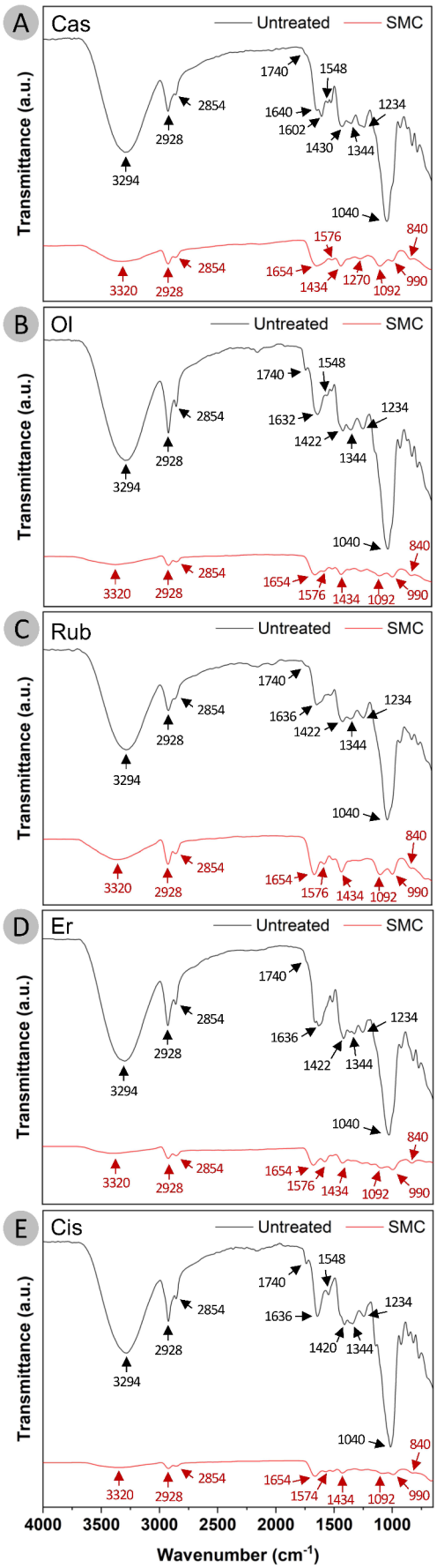

Fig. 7 FTIR spectra of raw bee pollen and purified SMCs with acetone, diethyl ether, and 85% H_3PO_4 (70 °C for 8 h). (**A**) *Castanea* spp. (Cas), (**B**) *Olea* spp. (Ol), (**C**) *Rubus* spp. (Rub), (**D**) *Erica* spp. (Er), and (**E**) *Cistus* spp. (Cis)

be altered by changing the temperature during purification [36], treating with UV-Ozone [20], or pH [38], thanks to the presence of functional groups in the chemical structure of sporopollenin. Our results for the water contact angle were similar to those reported for various SMCs in the literature [8, 20].

Thermal Evaluation

Sporopollenin biopolymer is resistant not only to harsh chemical conditions but also to heat changes. To understand the thermal resistance of the sporopollenin biopolymer-structured SMCs, they were heat treated up to 700 °C, Fig. 9, and compared to the raw material. Natural bee pollen profiled four major degradation steps during heating treatment, losing weight from 97% (Ol) to almost 100% (Rub) at the end of the analysis, Fig. 9A. This occurred in only three degradation steps for the purified SMCs, ranging from 93% (Cis) to 99% (Ol), Fig. 9D. The dTGs for both bee pollen and SMCs clearly elucidate the peaks associated with each weight loss during the thermal analysis, Fig. 9B and E. Additionally, percentage weight losses over certain temperature ranges can be found in Tables S3 and S4 for all samples.

For the bee pollen samples, the first weight loss between 21 °C and 110 °C is related to the evaporation of the weakly adsorbed water [31], while the second loss, between 110 °C and 260 °C, Fig. 9B, which is responsible for the loss of 31% (Ol) – 34% (Er) in weight, could be due to the degradation of proteins in natural bee pollen. It was previously stated by Ricci et al. [39] that the thermal decomposition temperature of proteins may vary between 178 °C and 288 °C, depending on their source and purity degree. The third stage decomposition, which occurs between 260 °C and 400 °C, accounts for a weight loss of 24% (Er) – 31% (Ol). These peaks were similar to the dTG decomposition peak seen in the *Lycopodium clavatum* pollen: a decomposition peak at 300 °C appeared in the study for the raw pollen grains, while the peak was missing for the acetone-treated (defatted) sample [36]. Thus, this phenomenon suggests that the decomposition peak around 300 °C may be due to the degradation of lipid compounds [36]. In the last stage, weight loss for the raw bee pollen occurred between 400 °C and 700 °C and appeared as two peaks in this range, except for the Er sample. These peaks account for weight loss of 32% (Ol) – 38% (Er) and may be associated with the partial decomposition of the exine layer and cellulose, which forms the inner layer of pollen grains [29, 35]. The weight losses at

this temperature agree with previously reported TGA findings for *Pinus* and *Tilia* pollen species [31].

For SMCs, weight reduction due to the evaporation of weakly adsorbed water was also observed at the initial heating stage until 200ºC, accounting for 4% (Er) to 10% (Cas) loss, Fig. 9E [40]. Relatively smaller peaks occurring at 200–400 °C are responsible for the weight loss in the second stage, resulting in mass loss of SMCs ranging from 47% (Cas) to 54% (Er). In this range, decomposition could be due to pectin and cellulose residues since the maximum decomposition temperatures of these biopolymers are 234 °C and 355 °C, respectively [35, 41, 42]. The third stage of weight loss at 400–700 °C accounts for the partial decomposition of the wall materials of the sporopollenin because after chemical treatment, the pollen is devoid of cellular components and consists mainly of sporopollenin [29, 31, 36, 40].

The thermal degradation profile for the purified SMCs showed a quite different pattern than that of natural pollen grains. This proves that protein, lipids, cellulose, and other pollen components were removed after defatting, H_3PO_4 treatment, and washings, resulting in a purer product [35, 40]. Moreover, the degradation of sporopollenin occurs at a higher temperature in natural bee pollen, indicating that the decomposition behaviour of pure components changes in the presence of other components [43]. Therefore, it seems reasonable to point out that the presence of pollen cellular materials and/or cellulose may alter the degradation behaviour of sporopollenin [36, 43].

To gain a deeper understanding of the thermal behaviour of the samples, we evaluated the thermal transitions that occur during heating with DTA, Fig. 9C and F. Natural bee pollen grains exhibited exothermic peaks at around 250–400 °C and endothermic peaks, along with exothermic peaks at 400–650 °C, Fig. 9C. For SMCs, slightly broader and sharper exothermic peaks were observed between 250 °C and 500 °C, Fig. 9F. These decomposition peaks were consistent with the weight loss regions of natural bee pollen and SMCs in the dTA thermograms. Thermal changes in treated and untreated samples are associated with the degradation of various pollen components in natural bee pollen and purified SMCs, such as lipids, proteins, cellulose, pectin, and sporopollenin [29, 31]. Protein content, SEM, CLSM, and FTIR results support the thermal analysis findings.

Conclusions

We have demonstrated how hollow microcapsules of a uniform size could be straightforwardly fabricated from different pollen species frequently available in natural environments, exploring honeybees and their appetence to collect pollen. SMCs were produced from renewable bee pollen pellets by a fast and unsophisticated chemical method, without the need for heavy chemical processes and complex instruments. SMCs produced this way offer some notable advantages over microcapsules harvested directly from plants or synthetically produced. Bee pollen pellets served as a green source for producing microcapsules with various surface architectures and apertures in the desired size in a short time and at a single place (e.g. in a beehive or apiary) and with fewer series of processes. With a well-defined chemical treatment method, we could fabricate five types of hollow SMCs with sizes ranging from ~12 to 36 µm, depending on the pollen species, without damaging their 3D micro- and nano-structures. SMCs with aliphatic and aromatic domains in their chemical structure showed different degrees of affinity for water and were thermally stable up to 451 °C. The pathway proposed here offers that

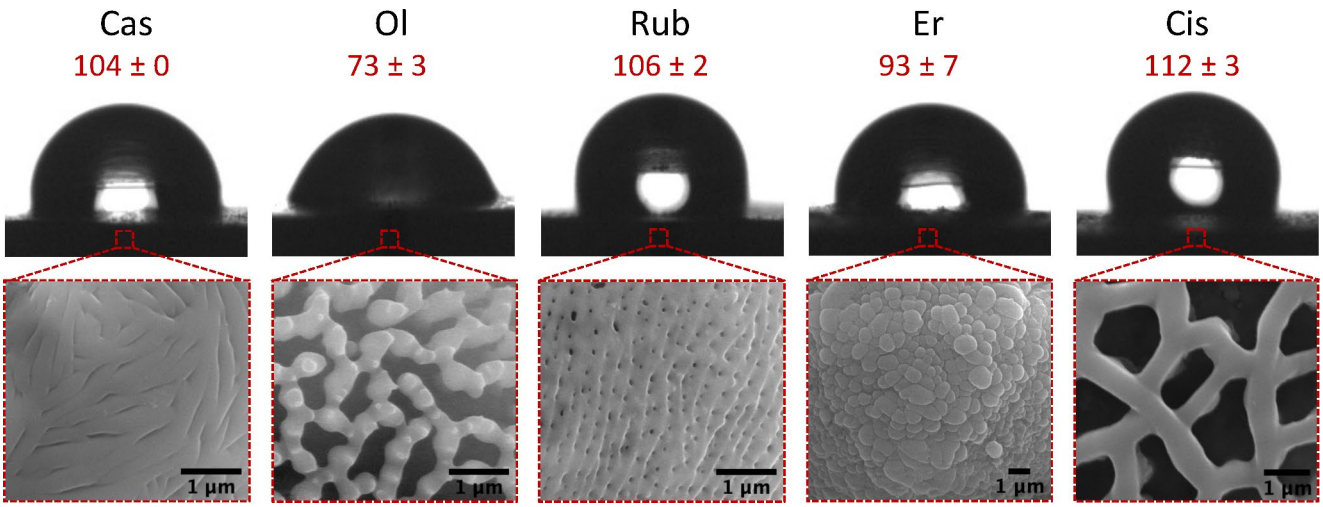

Fig. 8 Water contact angle measurements of the SMCs and surface morphology by SEM. *Castanea* spp. (Cas), (**B**) *Olea* spp. (Ol), (**C**) *Rubus* spp. (Rub), (**D**) *Erica* spp. (Er), and (**E**) *Cistus* spp. (Cis)

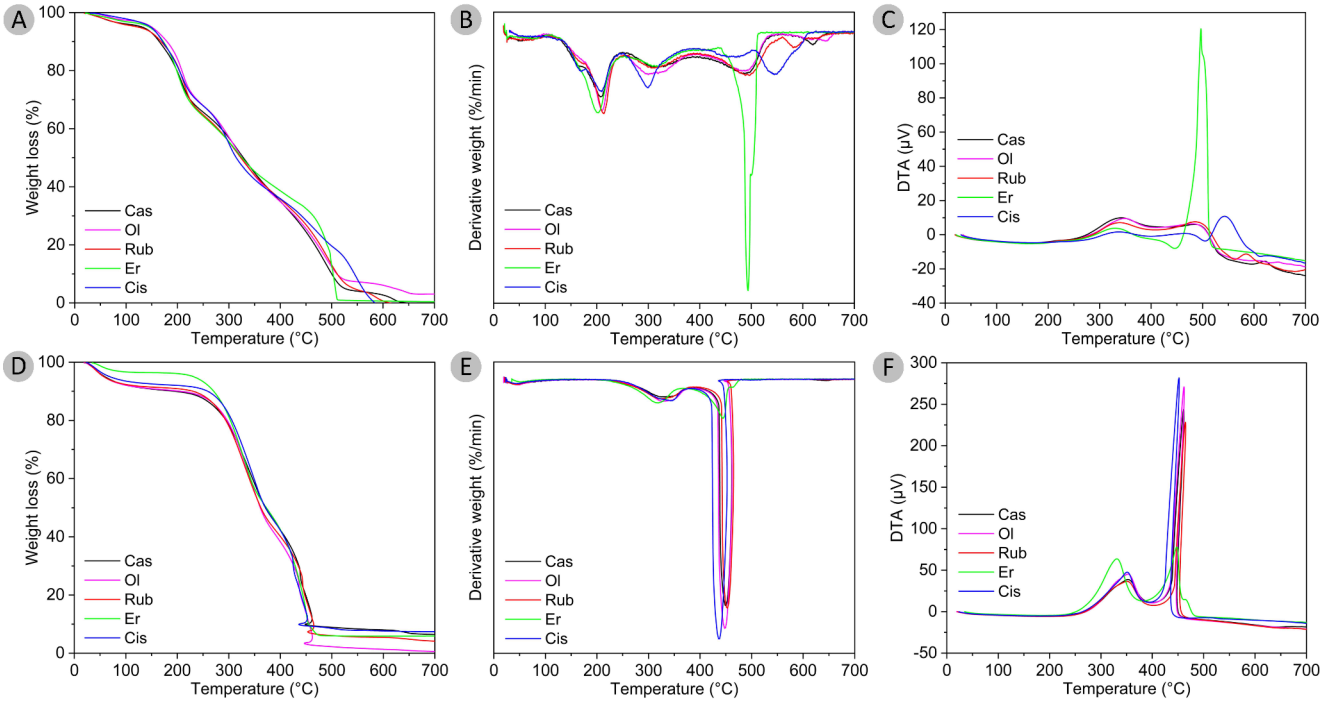

Fig. 9 Thermal behavior of bee pollen and SMCs. (**A**), (**B**) and (**C**) show TGA, dTG, and DTA thermograms for raw bee pollen, while (**D**), (**E**), and (**F**) are for SMCs, respectively. *Castanea* spp. (Cas), *Olea* spp. (Ol), *Rubus* spp. (Rub), *Erica* spp. (Er), and *Cistus* spp. (Cis)

micro-sized capsules can be straightforwardly produced and expands the range of natural materials that can be used for the sustainable development of green products of different sizes and shapes with useful properties in food, pharmaceutical, and biomedical applications.

Supplementary Information The online version contains supplementary material available at https://doi.org/10.1007/s10924-024-03478-0.

Acknowledgements The authors are grateful to the Foundation for Science and Technology (FCT, Portugal) for financial support by national funds FCT/MCTES to CIMO (UIDB/00690/2020 and UIDP/00690/2020), SusTEC (LA/P/0007/2021) and projects: UIDB/50006/2020, UIDB/04033/2020 and UIDP/50006/2020. Thanks to national funding, FCT for CEEC contract (2020.01614.CEECIND/CP1596/CT0007) with Andreia F. Peixoto and Ph.D. research grants for Seymanur Ertosun (2021.08361.BD) and Volkan Aylanc (2021.07764.BD). Thanks to the NextGenerationEU recovery funds, through the scope of Project BeeLand 10/C05-i03/2021.PPRR-C05-i03-I-000081.

Author contributions SE and VA: Investigation, Data Curation, Visualization, Writing—original draft. AP: Methodology, Data Curation and Writing—review. AS: Investigation, Data Curation and Writing—review. PR: Investigation, Data Curation and Writing—Review. CF: Conceptualization, Supervision, Funding acquisition and Writing—review, MV: Conceptualization, Supervision, Funding acquisition and Writing—review and editing.

Data Availability No datasets were generated or analysed during the current study.

Declarations

Competing Interests The authors declare no competing interests.

References

1. Aylanc V, Falcão SI, Ertosun S, Vilas-Boas M (2021) From the hive to the table: Nutrition value, digestibility and bioavailability of the dietary phytochemicals present in the bee pollen and bee bread. Trends Food Sci Technol 109:464–481. https://doi.org/10.1016/j.tifs.2021.01.042
2. Fan TF, Potroz MG, Tan EL, Ibrahim MS, Miyako E, Cho NJ (2019) Species-Specific Biodegradation of Sporopollenin-Based Microcapsules. Sci Rep 9:1–13. https://doi.org/10.1038/s41598-019-46131-w
3. Dobritsa AA, Nishikawa SI, Preuss D, Urbanczyk-Wochniak E, Sumner LW, Hammond A, Carlson AL, Swanson RJ (2009) LAP3, a novel plant protein required for pollen development, is essential for proper exine formation. Sex Plant Reprod 22:167–177. https://doi.org/10.1007/s00497-009-0101-8
4. Park JH, Seo J, Jackman JA, Cho NJ (2016) Inflated Sporopollenin Exine Capsules Obtained from Thin-Walled Pollen. Sci Rep 6:1–10. https://doi.org/10.1038/srep28017
5. Stamatopoulos K, Kafourou V, Batchelor HK, Konteles SJ (2021) Sporopollenin Exine Microcapsules as Potential Intestinal Delivery System of Probiotics. Small 17:2004573. https://doi.org/10.1002/smll.202004573
6. Raish M, Kalam MA, Ahmad A, Shahid M, Ansari MA, Ahad A, Ali R, Jardan YAB, Alshamsan A, Alkholief M, Alkharfy KM, Abdelrahman IA, Al-Jenoobi FI (2021) Eudragit-Coated Sporopollenin Exine Microcapsules (SEMC) of Phoenix dactylifera L. of 5-Fluorouracil for Colon-Specific Drug Delivery. Pharmaceutics 13:1921. https://doi.org/10.3390/pharmaceutics13111921

7. Diego-Taboada A, Sathyapalan T, Courts F, Lorch M, Almutairi F, Burke BP, Harris K, Kruusmägi M, Walther T, Booth J, Boa AN, Archibald SJ, Thompson C, Atkin SL, Mackenzie G (2022) Spore exines increase vitamin D clinical bioavailability by mucoadhesion and bile triggered release. J Controlled Release 350:244–255. https://doi.org/10.1016/j.jconrel.2022.08.017
8. Liu J, Yan XD, Li XQ, Du YH, Zhu LL, Ye TT, Cao ZY, Dong ZW, Li ST, Xu X, Bai W, Li D, Zhang JW, Wang SJ, Li SH, Sun J, Yin XZ (2023) Chrysanthemum sporopollenin: A novel vaccine delivery system for nasal mucosal immunity. Front Immunol 14:1132129. https://doi.org/10.3389/fimmu.2023.1132129
9. Aylanc V, Peixoto AF, Vale N, Freire C, Vilas-Boas M (2023) Sporopollenin-based bio-microcapsules as green carriers for controlled delivery of pharmaceutical drugs. Appl Mater Today 33:101860. https://doi.org/10.1016/j.apmt.2023.101860
10. Chandrasekaram K, Alias Y, Fathullah SF, Lee VS, Haron N, Raoov M, Zakaria N, Mohamad S (2021) Sporopollenin supported ionic liquids biosorbent for enhanced selective adsorption of 2,4-dinitrophenol from aqueous environment. Mater Today Commun 28:102587. https://doi.org/10.1016/j.mtcomm.2021.102587
11. Ávila-Avilés RD, Torres-Gómez N, Camacho-López MA, Vilchis-Nestor AR (2020) SERS activity of hybrid nano/microstructures Ag-Fe3O4 based on Dimorphotheca ecklonis pollen grains as bio-template. Sci Rep 10:1–9. https://doi.org/10.1038/s41598-020-73615-x
12. Cojocaru R, Mannix O, Capron M, Miller CG, Jouneau PH, Gallet B, Falconet D, Pacureanu A, Stukins S (2022) A biological nanofoam: The wall of coniferous bisaccate pollen. Sci Adv 8:892. https://doi.org/10.1126/sciadv.abd0892
13. Mundargi RC, Potroz MG, Park S, Park JH, Shirahama H, Lee JH, Seo J, Cho NJ (2016) Lycopodium Spores: A Naturally Manufactured, Superrobust Biomaterial for Drug Delivery. Adv Funct Mater 26:487–497. https://doi.org/10.1002/adfm.201502322
14. Deng Z, Pei Y, Wang S, Zhou B, Hou X, Li J, Li B, Liang H (2020) Designable Carboxymethylpachymaran/Metal Ion Architecture on Sunflower Sporopollenin Exine Capsules as Delivery Vehicles for Bioactive Macromolecules. J Agric Food Chem 68:13990–14000. https://doi.org/10.1021/acs.jafc.0c05169
15. Wei L, Tian K, Zhang X, Jin Y, Shi T, Guo X (2016) 3D Porous Hierarchical Microspheres of Activated Carbon from Nature through Nanotechnology for Electrochemical Double-Layer Capacitors. ACS Sustain Chem Eng 4:6463–6472. https://doi.org/10.1021/ACSSUSCHEMENG.6B01227/SUPPL_FILE/SC6B01227_SI_001.PDF
16. Baran T, Sargın İ, Kaya M, Mulerčikas P, Kazlauskaitė S, Menteş A (2018) Production of magnetically recoverable, thermally stable, bio-based catalyst: Remarkable turnover frequency and reusability in Suzuki coupling reaction. Chem Eng J 331:102–113. https://doi.org/10.1016/j.cej.2017.08.104
17. Tan EL, Potroz MG, Ferracci G, Jackman JA, Jung H, Wang L, Cho NJ (2018) Light-Induced Surface Modification of Natural Plant Microparticles: Toward Colloidal Science and Cellular Adhesion Applications. Adv Funct Mater 28:1707568. https://doi.org/10.1002/adfm.201707568
18. Hegedüs K, Fehér C, Jalsovszky I, Kristóf Z, Rohonczy J, Vass E, Farkas A, Csizmadia T, Friedbacher G, Hantz P (2021) Facile isolation and analysis of sporopollenin exine from bee pollen. Sci Rep 11:1–16. https://doi.org/10.1038/s41598-021-87619-8
19. Fan TF, Hwang Y, Potroz MG, Lau KL, Tan EL, Shahrudin Ibrahim M, Miyako E, Cho NJ (2020) Degradation of the sporopollenin exine capsules (SECs) in human plasma. Appl Mater Today 19:100594. https://doi.org/10.1016/j.apmt.2020.100594
20. Tan EL, Potroz MG, Ferracci G, Wang L, Jackman JA, Cho NJ (2020) Hydrophobic to superhydrophilic tuning of multifunctional sporopollenin for microcapsule and bio-composite applications. Appl Mater Today 18:100525. https://doi.org/10.1016/j.apmt.2019.100525
21. Cane JH, Tepedino VJ (2017) Gauging the Effect of Honey Bee Pollen Collection on Native Bee Communities. Conserv Lett 10:205–210. https://doi.org/10.1111/conl.12263
22. Louveaux J, Maurizio A, Vorwohl G (2015) Methods of Melissopalynology. Bee World 59:139–157. https://doi.org/10.1080/00057772X.1978.11097714
23. Von Der Ohe W, Persano Oddo L, Piana ML, Morlot M, Martin P (2004) Harmonized methods of melissopalynology. Apidologie 35:18–25. https://doi.org/10.1051/apido:2004050
24. AOAC (2016) Official Methods of Analysis of AOAC INTERNATIONAL, 20th edn. AOAC International, Gaithersburg
25. de Carvalho AS, de Rezende SC, Caleja C, Pereira E, Barros L, Fernandes I, Manrique YA, Gonçalves OH, Ferreira ICFR (2021) Barreiro, β-Carotene colouring systems based on solid lipid particles produced by hot melt dispersion. Food Control 129:108262. https://doi.org/10.1016/j.foodcont.2021.108262
26. Uddin MJ, Gill HS (2017) Ragweed pollen as an oral vaccine delivery system: Mechanistic insights. J Controlled Release 268:416–426. https://doi.org/10.1016/j.jconrel.2017.10.019
27. Fan T, Park JH, Pham QA, Tan EL, Mundargi RC, Potroz MG, Jung H, Cho NJ (2018) Extraction of cage-like sporopollenin exine capsules from dandelion pollen grains. Sci Rep 8:1–11. https://doi.org/10.1038/s41598-018-24336-9
28. Uddin MJ, Gonzalez-Cruz P, Warzywoda J, Gill HS (2020) Sporopollenin Spikes Augment Antigen-Specific Immune Response and Generate Long-Lived Humoral Immunity. Adv Ther (Weinh) 3:2000102. https://doi.org/10.1002/adtp.202000102
29. Alpizar-Reyes E, Concha JL, Martín-Martínez FJ, Norambuena-Contreras J (2022) Biobased Spore Microcapsules for Asphalt Self-Healing. ACS Appl Mater Interfaces 14:31296–31311. https://doi.org/10.1021/acsami.2c07301
30. Uddin MJ, Liyanage S, Warzywoda J, Abidi N, Gill HS (2022) Role of Sporopollenin Shell Interfacial Properties in Protein Adsorption. Langmuir 38:2763–2776. https://doi.org/10.1021/acs.langmuir.1c02682
31. Atalay FE, Culum AA, Kaya H, Gokturk G, Yigit E (2022) Different Plant Sporopollenin Exine Capsules and Their Multifunctional Usage. ACS Appl Bio Mater 5:1348–1360. https://doi.org/10.1021/acsabm.2c00071
32. Jardine PE, Abernethy FAJ, Lomax BH, Gosling WD, Fraser WT (2017) Shedding light on sporopollenin chemistry, with reference to UV reconstructions. Rev Palaeobot Palynol 238:1–6. https://doi.org/10.1016/j.revpalbo.2016.11.014
33. Lutzke A, Morey KJ, Medford JI, Kipper MJ (2020) Detailed characterization of Pinus ponderosa sporopollenin by infrared spectroscopy. Phytochemistry 170:112195. https://doi.org/10.1016/j.phytochem.2019.112195
34. Chiappe C, Rodriguez-Douton MJ, Mozzati MC, Prete D, Griesi A, Guazzelli L, Gemmi M, Caporali S, Calisi N, Pomelli CS, Rossella F (2020) Fe-functionalized paramagnetic sporopollenin from pollen grains: one-pot synthesis using ionic liquids. Sci Rep 10:1–10. https://doi.org/10.1038/s41598-020-68875-6
35. Uddin MJ, Liyanage S, Abidi N, Gill HS (2018) Physical and Biochemical Characterization of Chemically Treated Pollen Shells for Potential Use in Oral Delivery of Therapeutics. J Pharm Sci 107:3047–3059. https://doi.org/10.1016/j.xphs.2018.07.028
36. Uddin MJ, Abidi N, Warzywoda J, Gill HS (2019) Investigation of the Fate of Proteins and Hydrophilicity/Hydrophobicity of Lycopodium clavatum Spores after Organic Solvent-Base-Acid Treatment. ACS Appl Mater Interfaces 11:20628–20641. https://doi.org/10.1021/acsami.9b03040
37. Huhtamäki T, Tian X, Korhonen JT, Ras RHA (2018) Surface-wetting characterization using contact-angle measurements. Nat Protoc 13:1521–1538. https://doi.org/10.1038/s41596-018-0003-z

38. Li D, Sun L, Shi L, Zhuo L, Yang L, Zhang J, Han Y, Ye T, Wang S (2023) Reversible switchable wettability of intrinsic micro/nanostructured pollen microcarriers via pH-induce from superhydrophobicity to superhydrophilicity. Chem Eng J 473:145184. https://doi.org/10.1016/j.cej.2023.145184
39. Ricci L, Umiltà E, Righetti MC, Messina T, Zurlini C, Montanari A, Bronco S, Bertoldo M (2018) On the thermal behavior of protein isolated from different legumes investigated by DSC and TGA. J Sci Food Agric 98:5368–5377. https://doi.org/10.1002/jsfa.9078
40. Mohammed ASY, Dyab AKF, Taha F, Abd El-Mageed AIA (2022) Pollen-derived microcapsules for aspirin microencapsulation: in vitro release and physico-chemical studies. RSC Adv 12:22139–22149. https://doi.org/10.1039/D2RA02888C
41. Einhorn-Stoll U, Kunzek H (2009) The influence of the storage conditions heat and humidity on conformation, state transitions and degradation behaviour of dried pectins. Food Hydrocoll 23:856–866. https://doi.org/10.1016/j.foodhyd.2008.05.001
42. Yang H, Yan R, Chen H, Lee DH, Zheng C (2007) Characteristics of hemicellulose, cellulose and lignin pyrolysis. Fuel 86:1781–1788. https://doi.org/10.1016/j.fuel.2006.12.013
43. Burhenne L, Messmer J, Aicher T, Laborie MP (2013) The effect of the biomass components lignin, cellulose and hemicellulose on TGA and fixed bed pyrolysis. J Anal Appl Pyrol 101:177–184. https://doi.org/10.1016/j.jaap.2013.01.012